Lawrence Berkeley National Laboratory
LBL Publications

Title

Factors Affecting Indoor Air Concentrations of Volatile Organic Compounds at a Site of Subsurface Gasoline Contamination

Permalink

https://escholarship.org/uc/item/2nm1z33z

Authors

Fischer, M L
Bentley, A J
Dunkin, K A
et al.

Publication Date

1995-11-01

Copyright Information

Lawrence Berkeley Laboratory
UNIVERSITY OF CALIFORNIA

ENERGY & ENVIRONMENT DIVISION

Factors Affecting Indoor Air Concentrations of Volatile Organic Compounds at a Site of Subsurface Gasoline Contamination

M.L. Fischer, A.J. Bentley, K.A. Dunkin, A.T. Hodgson, W.W. Nazaroff, R.G. Sextro, and J.M. Daisey

November 1995
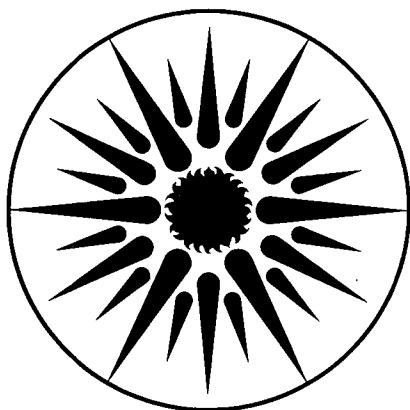
ENERGY AND ENVIRONMENT DIVISION

DISCLAIMER

FACTORS AFFECTING INDOOR AIR CONCENTRATIONS OF VOLATILE ORGANIC COMPOUNDS AT A SITE OF SUBSURFACE GASOLINE CONTAMINATION

Marc L. Fischer,[1] Abra J. Bentley,[1] Kristie A. Dunkin,[2] Alfred T. Hodgson,[1] William W. Nazaroff,[1,3] Richard G. Sextro,[1] Joan M. Daisey[1]

[1]Indoor Environment Program
E. O. Lawrence Berkeley National Laboratory
University of California
Berkeley CA 94720

[2]Department of Environmental Science Policy and Management
University of California
Berkeley CA 94720.

[3]Department of Civil and Environmental Engineering
University of California
Berkeley CA 94720-1710

November 1995

FACTORS AFFECTING INDOOR AIR CONCENTRATIONS OF VOLATILE ORGANIC COMPOUNDS AT A SITE OF SUBSURFACE GASOLINE CONTAMINATION

Marc L. Fischer,[1] Abra J. Bentley,[1] Kristie A. Dunkin,[2] Alfred T. Hodgson,[1] William W. Nazaroff,[1,3] Richard G. Sextro,[1] Joan M. Daisey[1]

[1]Indoor Environment Program,
E. O. Lawrence Berkeley National Laboratory
1 Cyclotron Rd, Berkeley CA 94720

[2]Department of Environmental Science Policy and Management
University of California
Berkeley CA 94720

[3]Department of Civil and Environmental Engineering
University of California
Berkeley CA 94720-1710

Abstract

We report a field study of soil gas transport of volatile organic compounds (VOCs) into a slab-on-grade building found at a site contaminated with gasoline. Although the high VOC concentrations (30-60 g m^{-3}) measured in the soil gas at depths of 0.7 m below the building suggest a potential for high levels of indoor VOC, the measured indoor air concentrations were lower than those in the soil gas by approximately six orders of magnitude ($\sim$ 0.03 mg m^{-3}). This large ratio is explained by 1) the expected dilution of soil gas entering the building via ambient building ventilation (a factor of $\sim$ 1000), and 2) an unexpectedly sharp gradient in soil gas VOC concentration between the depths of 0.1 and 0.7 m (a factor of $\sim$ 1000). Measurements of the soil physical and biological characteristics indicate that a partial physical barrier to vertical transport in combination with microbial degradation provides a likely explanation for this gradient. These factors are likely to be important to varying degrees at other sites.

Introduction

Soil gas transport of volatile organic contaminants (VOCs) into buildings has been documented as a potentially significant source of human exposure to VOCs (1-4). The volatile components of gasoline and other petroleum hydrocarbons are of concern because of the large number of storage tanks that are expected to be leaking (5), and previous studies reporting indoor air contamination (6, 7).

Estimation of indoor air VOC concentrations due to subsurface sources provides an important input when assigning priorities for remediation activities. Purely theoretical estimates of the expected levels of exposure due to the subsurface-to-indoor-air pathway are, however, highly dependent on the sophistication of the models and assumptions used in the estimates, with the results of different studies varying by many orders of magnitude (8-10). In particular, the large number of variables that control vapor phase transport and fate of subsurface contaminants into buildings can make prediction of the resulting indoor-air concentrations problematic. This suggests that screening measurements at sites in question are well advised (11).

This paper reports the results of a detailed experimental investigation of the physical and biological factors affecting gasoline vapor transport from contaminated soils into a building. The following sections describe the site and the type of contamination that occurred, the measurements of indoor air and soil gas VOC concentrations, the field and laboratory measurements performed to identify the factors affecting transport into the building, and a discussion of the relevance of these findings to other sites.

Site Description

This study was conducted at the site of a former gasoline station located at the Alameda Naval Air Station (ANAS), California (see Figure 1). Operation of the station began in the early 1970s. In 1980, one of three 45 m^3 underground storage tanks was damaged. The tank was drained and repaired in the period between 1980 and 1987. Subsequent tests revealed that subsurface leakage continued to be a problem, and in 1988 fuel was removed from the tanks and

the station was closed. In 1990 a soil gas survey detected high levels of gasoline hydrocarbon vapors in the soil (12).

The service station building was a single story slab on grade building with a flat roof. The building walls were constructed of hollow concrete masonry units (cinder blocks). The building contained a main office, two adjoining rooms, and two restrooms which have outside entrances. The building volume and floor area were $V = 120$ m^3 and $A = 50$ m^2 respectively. The building was not used for automotive service or repair and is therefore unlikely to have been directly contaminated with spilled petroleum hydrocarbons that might produce a high VOC background indoors. The soil underlying the site to depths of 2.5 to 4 m is hydraulic fill consisting of material ranging from sandy clay to coarse sand. Silty sand underlies the fill. The water table is located at a depth that lies between 1 and 3 m below the soil surface, varying in response to local precipitation.

Measurements

The field work at the ANAS site was performed from November 1993 to January 1995, with most of the measurements taken from July to October of 1994. Initially indoor air and soil gas VOC concentrations were measured. High concentrations of VOCs were measured in the soil gas while low concentrations were measured in the building. Subsequent work focused on determining the factors controlling VOC transport and entry into the building.

VOC constituents in outdoor air, indoor air, soil gas, and ground water

Samples of outdoor and indoor air were collected into Tedlar® bags using peristaltic pumps. Sample volumes of 3 liters were collected over the period of 4 hours near midday during clear weather. Soil gas was collected from locations beneath the building slab. Holes were drilled through the slab and 6 mm diameter stainless steel probe tubes were driven into the soil using a steel mandrel (to prevent clogging) and a hammer. The depths of the probes ranged from 0.1 to 2.1 m below the bottom of the concrete floor slab (the slab thickness was approximately 0.1 m). Because of the soil texture, the small probe tube diameters, and the relatively shallow depths, drilling tap holes in the soil was not required. After installation, the probes were capped

and the holes through the slab were sealed with concrete so that no additional pathway for soil-gas entry was created. Soil gas volumes of 150 ml were drawn into Tedlar® bags from the probes at a rate of 100 cm^3 min^{-1}, after purging a minimum of two probe volumes (~20 ml), using a peristaltic pump. Similarly, a sample of contaminated ground water was collected from the deepest probe at a depth of 2.1 m.

Soil-gas and indoor air samples were analyzed using a gas chromatograph/mass spectrometer (GC/MS). As configured, the GC/MS was capable of detecting compounds heavier than propane. Measured sample volumes, chosen to produce measurable signals but not overload the GC/MS, were transferred from the Tedlar® bags to multi-sorbent sample tubes (13). The sorbent tubes were also injected with 125 ng bromofluorobenzene (BFB) as a calibration standard. The gas samples plus BFB were then introduced into the GC using a thermal-desorption concentrator system. The fractional variation in the area of the BFB calibration signal among samples was typically between 0.05 and 0.10. Peaks in the ion-mass chromatogram were identified using the EPA/NIH mass spectral data base. The concentrations of identified compounds were estimated from the integrated total ion-mass signal relative to that for the BFB. This calibration scheme produced fractional errors of less than 0.2 of the true concentrations for known test samples of aliphatic and aromatic hydrocarbons.

Samples of outdoor and indoor air, soil gas sampled at depths of 0.1 and 0.7 m relative to the bottom of the slab, and the headspace vapor above the ground water sample were analyzed. The samples contained a large number of compounds typically found in gasoline vapor. Table 1 lists seven dominant constituents detected in GC/MS analysis, as well as benzene and toluene. The indoor air VOC concentrations in excess of those expected from outdoor air, and therefore attributed to soil-gas entry into the building, were estimated as the indoor minus outdoor concentrations. Of the VOCs likely to be the result of soil-gas entry into the building, 2 methyl butane (isopentane, henceforth isoP) was detected with the highest concentrations in both the soil gas and indoors. isoP is also a major volatile constituent of gasoline vapor, and has relatively low solubility in water (14). In the subsequent work we used isoP as a tracer for gasoline vapor.

4

This had the advantage that larger numbers of rapid measurements could be made with low volume soil gas samples using less expensive detection equipment, but had the disadvantage that the transport and fate of other VOCs in the soil gas were not characterized.

Depth profiles of soil gas isoP, CH_4, O_2, and CO_2

Measurements of the depth profiles of isoP and other selected soil gas constituents were performed in July, August, and October of 1994. Soil gas was sampled from a cluster of probes (SG 1-6) terminating at depths of 0.1, 0.4 , 0.65 , 0.9 , 1.3, and 1.6 m below the bottom of the slab. Samples volumes of 150 cm^3 were pumped into Tedlar® bags as described above. Analysis was performed using a gas chromatograph equipped with two gas sampling loops and GC columns, one that fed a photoionization (PID) / flame ionization (FID) detector combination, and a second that fed a thermal conductivity detector(TCD). The FID was used to measure isoP and the total amount of volatile organic carbon burned in the FID (TVOC), while the TCD was used to measure CH_4, O_2, and CO_2. A calibration standard was prepared that contained each of the gases being measured. The fractional run-to-run repeatability of the calibration standard was better than 0.15 for all gases. During the first set of measurements, the ratio of PID/FID signals was examined to detect the presence of benzene and toluene, but yielded no significant detections of these gases. Figure 2 shows the results of a typical soil gas measurement. During the four month period, the measured concentrations of all species varied by less than a factor of two about the concentrations reported in Figure 2. An unexpected result was the very sharp gradient in organic vapor concentrations that were measured between the depths of 0.4 and 0.65 m. While the O_2 concentration decreased by approximately a factor of three from that of outdoor air, isoP and CH_4 increased by two orders of magnitude, and CO_2 by a factor of four.

Soil physical and chemical properties

Soil properties were determined from core samples collected in July 1994 from a boring made through the building slab one meter East of the cluster of probes SG 1-6, shown in Figure 1. A bucket auger was used to clear the hole to a given depth and then a stainless steel coring tool was driven into the soil. Individual soil cores measured 5.4 cm in diameter by 6 cm

long. Cores were collected from depths ranging from 0.3 to 2 m below the slab. The soil at depths less than 0.2 m was dominated by sandy gravel which made intact soil cores impossible to collect. After the cores were removed, the entire boring hole and the hole in the building slab were filled with concrete. Standard soil analysis techniques were performed on the soil cores to determine the dry soil density, total and air filled porosities, and the fractions of silt, clay, organic carbon, and moisture relative to dry soil (15). We note that the estimate of organic carbon should be considered a lower limit because it was measured after the soil was oven dried for 24 hours at a temperature of 80 ° C, and the volatile organic compounds were probably lost. A summary of these results is reported in Table 2. The pH of the soil was measured separately. Using a standard analysis (15), the average pH values were 7.2, 8.1, and 8.4, for soil samples collected at depths of 0.2-0.4, 0.5-0.7, and 0.9-1.1 m respectively.

Visual inspection of the cores revealed relatively uniform light colored sand mixed with bits of shells, with a slightly darker layer at a depth of 0.6 m and then a transition to a darker greenish sand, indicative of anaerobic conditions, at greater depths. The soil size fraction is dominated by sand with small fractions of silt and clay that increase slowly with depth. The average total soil porosity of 0.38 is consistent with soil type. An interesting feature is the increase in soil moisture and organic carbon content at depths of 0.58, 0.62 and 0.7 m.

Soil permeability to air was measured in the soil under the building, and in the uncovered soil directly adjacent to the building using two techniques. In addition to the smaller soil gas probes, five probes with inside diameters of 1 cm (not shown in Figure 1) were installed under the slab terminating at depths between 0.6 and 1 m. Soil gas was pumped out of the probes and the volumetric flow rate was measured as a function of applied pressure. In all cases, the flow was measured to be proportional to the pressure, suggesting that transport was determined by Darcy flow in the soil (16). These measurements yield soil permeabilities that are heavily weighted by the permeability within approximately 0.1 m of the probe tip (17), and range from 1-3 x 10^{-12} m^2. Outside the building a dual probe dynamic pressure technique, described by Garbesi et al. (17), was used to measure the air permeability of the soil over a range of length

6

scales up to 4 m. The permeabilities measured next to the building on 0.1 m scales matched those measured under the building. However, the permeability measured on scales larger than 1 m, which are most appropriate for estimating soil gas transport into this building, were approximately 10^{-11} m^2 (17).

The depth of the water table was measured in a shallow well, drilled directly adjacent to the building (Figure 1). The depth varied significantly on long time scales and appears to be driven by the amount of rain the site receives. The depth was 1.9 m in July 1994 when the soil cores were collected, varying to a maximum of 2.5 m in October 1994, and a minimum of 1.0 m in January 1995 after a series of heavy rains. In addition to the long term measurements, we also measured the water depth over a 12 hr period during a full moon to estimate the influence of tidal variation on the water table. No significant (< 1 cm) variation was observed. Longer term measurements at another nearby site showed similar results (18).

Tracer gas transport in soil

Measurements of soil gas transport were conducted to help understand the observed gradient in soil-gas concentrations. A one-liter volume of air containing a 0.01 volume fraction of sulfur hexafluoride (SF$_6$) was injected into the soil at a depth of 0.75 m at the location marked as SF$_6$(1) in Figure 1. The concentration of SF$_6$ was then monitored at the other soil gas probes at regular intervals for 55 days. Soil gas samples were collected from each of the probes using 30 ml plastic syringes. Two probe volumes were removed before the samples were collected. The SF$_6$ concentrations were analyzed using a GC equipped with an electron capture detector (ECD). Calibrations were performed before each run with a fractional run-to-run repeatability of 0.1. The detection limit for SF$_6$ was 0.5 ppb.

The results of the tracer gas measurements are shown in Figures 3 and 4. Although relatively little transport occurred in the upward direction from the injection point to depths less than 0.5 m, the SF$_6$ dispersed rapidly in the horizontal and downward directions. Because the sorption and degradation of SF$_6$ in soil are negligible, the measured anisotropy in transport

7

suggested that a partial barrier to vertical transport existed in the soil at depths between 0.4 and 0.65 m.

A second SF_6 tracer gas test was performed as part of the measurements to determine the soil gas coupling to indoor air and to examine vertical transport in the soil gas. One-liter of pure SF_6 was injected into the soil immediately below the slab at each of the four locations marked as $SF_6(2)$ in Figure 1. After 21 days, soil gas samples were collected from the cluster of probes SG 1-6. A strong gradient with depth was observed; high concentrations of 200 ± 10 ppm were measured in the probes at depths of 0.1 and 0.4 m, while low concentrations of 21 ± 2 ppm were measured in the probes at 0.6, 0.9, and 1.3 m, supporting the notion of a partial barrier to vertical transport.

[222]Radon measurements

[222]Rn concentrations were measured in the soil gas as a function of depth. Soil gas was collected from probes at several depths and locations under the building. Sampling was performed twice, once in August and again in October, 1994. Samples were pumped through a filter to remove [222]Rn decay products into scintillation flasks and counted with a photomultiplier (19). The average [222]Rn concentrations in the subslab (depths of 0.1 to 0.4 m) and deep soil (depths > 0.65 m) were $C_{Rn}(subslab) = 5000 \pm 750$ Bq m^{-3} and $C_{Rn}(deep) = 9300 \pm 600$ Bq m^{-3}, respectively.

Building ventilation and soil gas infiltration

The building ventilation rate, Q_v (m^3 d^{-1}), was measured as a function of an imposed building depressurization, ΔP (Pa), using a fan designed for testing ventilation ducts. The pressure difference across the building shell was varied from 0 to 75 Pa. The measured data are well fit ($R^2 = 0.98$) by a power law:

$$Q_v = Q_0 \, (\Delta P / 1 \, Pa)^n \quad (m^3 \, d^{-1}), \tag{1}$$

where $Q_0 = 3300$ m^3 d^{-1} and n = 0.59. The estimated average ventilation rate of 0.6 air changes per hour is in the range expected for a building of this size and type (20).

Soil-gas entry into the building was estimated using SF_6 in the soil gas as a tracer. Two sets of measurements were conducted at different building depressurizations. First, the indoor SF_6 concentration resulting from weather-induced entry was measured under ambient conditions. The building was not heated or actively ventilated during this time. During this test in October, 1994 the average outdoor temperature was approximately 15° C, and the dominant source of depressurization was wind loading on the building. Two weeks after SF_6 was injected into the soil immediately below the slab (as described above), a 1 liter sample of indoor air was continuously pumped into a Tedlar® bag for one week. The concentration of SF_6 in the one-week average was 50 ppb. At the end of the one week sample period the soil-gas concentration of SF_6 was measured to be 200 ± 10 ppm in the cluster of probes SG 1-6 at depths of 0.1 and 0.4 m. Immediately following the first test , the second test was conducted by actively depressurizing the building to 10 and 75 Pa, and measuring the SF_6 concentration in the air at the exhaust fan. The measured SF_6 concentrations were 90 ± 10 ppb at both depressurizations.

Laboratory test of potential for biodegradation

The measured gradients of hydrocarbons, O_2 and CO_2 in soil gas are suggestive of aerobic consumption of the hydrocarbons by soil microorganisms. An *in situ* test for estimating total rates of hydrocarbon degradation, described by Hinchee & Ong (21), was considered but the sharpness of the gradients appeared to limit the applicability of the technique. Instead, we choose to perform a laboratory incubation experiment to measure the rate of isoP consumption in soil samples containing the indigenous microorganisms and soil nutrients.

. Soil core samples were collected from depth intervals of 0.2-0.4 and 0.5-0.7 m, and stored at a temperature of 15° C. Two duplicate soil sub-samples and a third sterilized soil sample, intended as a control, from each depth interval were introduced into separate 250 ml sterilized amber bottles and sealed with Mininert® caps with syringe septa. The equivalent mass of dry soil was 10 g in all cases. The soil controls were sterilized by repeated autoclaving and then rehydrated with 1 g sterile water. All of the soil samples and two empty bottles (blanks) were injected with 12.5 mg isoP. The resulting initial concentration of isoP in the bottle

headspace, $C_{isoP}(t=0) = 50$ g m^{-3}, was chosen to approximate the average concentration of isoP in the deep soil gas samples. The bottles were then placed in a water bath at 20° C. The isoP headspace concentrations were measured regularly over the course of the 450 hr experiment by removing 20 µl gas samples that were then analyzed using the GC/FID described above. At the end of the experiment, headspace concentrations of CH_4, CO_2, O_2 were measured to determine the stoichiometry of any reactions that might have occurred.

Figure 5 shows the isoP headspace concentrations as a function of time for the active soil samples, the controls, and the blanks. After an initial period (lag phase) of approximately 80 hours, during which we assume the microbial population was increasing, the isoP concentration in the active soil samples dropped. The most rapid and complete consumption occurred in the bottles containing the 0.2-0.4 m depth soil samples. The stoichiometry results from the final measurements of isoP, CO_2, O_2 are given in Table 3 as changes in their molar concentrations. No residual hydrocarbons other than isoP were detected in any of the bottles. With the exception of O_2, none of the gases changed significantly in either the blanks or the soil controls. If one assumes that half of the isoP consumed is converted to biomass (21) and the other half is converted to CO_2 and H_2O, then one expects $\Delta CO_2 \approx -2.5$ x $\Delta isoP$, and $\Delta O_2 \approx 4$ x $\Delta isoP$. Examination of the data from both depths shows that the changes in isoP, CO_2, and O_2 agree with the above estimates to within 20%.

Analysis

In this section we describe a conceptual model for the transport of contaminants from the soil gas into the building, and use it to interpret the measured data. Figure 6 shows a schematic cross-sectional view of the building and surrounding soil that illustrates the model, and the equivalent three box model. Contaminant transport is assumed to occur by diffusion from the deep soil upward toward the building. At depths between 0.4 and 0.65 m, a low-diffusivity soil layer restricts the flow, generating the gradients in contaminants, CO_2, and O_2 shown in Figure 2. Just above the low-diffusivity layer we assume there is an aerobic microbial population in the sub-slab region that consumes a fraction of the contaminants that cross the layer. The remaining

10

contaminants are carried out of the sub-slab region and into the building by advection of outdoor air flowing through the soil near the building foundation and into the building, and by molecular diffusion through the soil and building slab. The advective flows are caused by atmospheric pressure fluctuations and wind loading on the building (22, 23). Finally, wind loading pressurizes the soil surface on the upwind side of the building relative to the downwind side, driving a low-velocity "upwind-downwind" advective air flow into the soil on the upwind side, through the soil in both the sub-slab and deep regions, and out into the outdoor air on the downwind side.

The measured data are evaluated within the context of the three box model by assuming a mass balance first between entry into the building and removal from the subslab region, and second between entry into the subslab soil gas and transport out of the deep soil gas. This evaluation has four steps, each of which is described in detail below. 1) Using the measurements of building ventilation rate and SF_6 concentration we estimate the effective rate of soil-gas entry into the building (we also justify the assumption that removal rates in the sub slab and deep soil gas due to upwind-downwind advection are small compared to the vertical transport). 2) Using the gradient in SF_6 measured during the first tracer gas test, we estimate the vertical diffusive transport of SF_6 from the deep soil gas, through the low diffusivity layer, and into the sub-slab soil gas . 3) Assuming that this SF_6 flux is indicative of the diffusivity for other gas species, we estimate the rate of biodegradation necessary to produce the gradient actually observed in isoP. 4) We compare the estimated rate of isoP biodegradation with that observed in the laboratory incubation experiment.

Estimated effective soil-gas entry into building

The estimate of the effective soil-gas entry rate assumes a mass balance between contaminant entry into the building due to advection and diffusion and removal out of the building by building ventilation. Combining the effects of advection and diffusion, this mass balance can be written in terms of an effective entry rate

$$Q_{eff} = Q_v \, C(indoor)/C(subslab) \ (m^3 \ d^{-1}), \qquad (2)$$

11

where Q_v is the building ventilation rate from Eq (1), and the C(indoor)/C(subslab) is the ratio of contaminant concentrations in the indoor air to sub-slab soil gas. The combination of advective and diffusive transport is justified in this case because the indoor concentrations are generally much smaller than those in the sub-slab region so that both advective and diffusive entry are proportional to the sub-slab concentration. We note that combining the advective and diffusive terms yields a non-zero effective rate of contaminant entry into the building at zero building depressurization due to the diffusion term.

Evidence for this mass balance under ambient conditions is provided by the fact that the measured ratios of indoor to sub-slab soil-gas concentrations are approximately equal for isoP and SF_6. In the case of isoP (see Table 1), the ratio of indoor air concentration (attributed to soil-gas entry) to soil-gas concentration at a depth of 0.1 m was

$(C_{isoP}(indoor) - C_{isoP}(outdoor)) / C_{isoP}(subslab) = 25 \ \mu g \ m^{-3} / {\sim}100 \ mg \ m^{-3} = 3 \times 10^{-4}$. Similarly, in the case of the second SF_6 tracer gas measurement, the ratio was $C_{SF6}(indoor)/C_{SF6}(subslab)$ = 50 ppb/200 ppm = 3×10^{-4}. The building ventilation rate under ambient conditions can be estimated by assuming that the building depressurization is in the range $\Delta P \approx$ 1-5 Pa when the building is not actively heated or ventilated. Based on the fan depressurization tests described earlier, the corresponding ventilation rate is $Q_v \approx$ 3000-9000 $m^3 \ d^{-1}$. Thus the average effective soil-gas entry rate estimated from Eq (1) is $Q_{eff} \approx$ 1-3 $m^3 \ d^{-1}$.

Two checks for consistency were performed. First, we estimated the ambient building depressurization due to wind loading on the building. The depressurization due to wind loading is commonly estimated as a fraction (typically 0.2-0.3) of the Bernoulli pressure $P = 1/2 \ \rho_a <v^2>$, where ρ_a is the density of air, and $<v^2>$ is the square of the average wind speed (24). Data supplied by the meteorologist at ANAS show that the wind is relatively constant from the north to west with an average speed $<v>$ = 5.2 m s^{-1} at a height of 10 m, with occasional shifts to winds from the east during the summer. This suggests that the expected depressurization of the building is $\Delta P \approx$ 3 Pa, generally supporting the assumption made above.

12

Using the wind data we also estimated the magnitude and direction of the soil-gas velocity due to upwind-downwind pressure gradient, and the resulting volumetric flow rate. We assumed that the soil surface on the upwind side of the building was pressurized to the Bernoulli pressure while the soil surface on the downwind side was depressurized by the same amount (23). The resulting upwind-downwind velocity in the soil gas was estimated as the one-dimensional Darcy velocity

$$v_d = k/\mu \; dP/dx \approx 0.1 \text{ m d}^{-1}, \tag{3}$$

where the measured soil permeability to air, $k = 10^{-11} \text{ m}^2$, the viscosity of air $\mu = 1.8 \times 10^{-5}$ Pa s, and the expected pressure gradient due to wind loading $dP/dx \approx 2$ Pa m^{-1} oriented from the northwest. Assuming that the soil gas has this velocity in the sub-slab soil, one can estimate the volumetric flow rate in the sub-slab region

$$Q_{wind} = \varepsilon_a \, v_d \, l \, \Delta z \approx 0.1 \text{ m}^3 \text{ d}^{-1}, \tag{4}$$

where $\varepsilon_a \approx 0.22$ is the air-filled porosity of the soil in the subslab area, $l \approx 7$ m is an average cross sectional length under the building, and $\Delta z \approx 0.5$ m is the depth of the subslab region. Thus the removal of soil gas from the sub-slab region due to upwind-downwind advective flows is small compared to the estimated rate of soil-gas entry into the building.

Second, we estimated the effective rate of soil gas entry into the building under ambient conditions using the ^{222}Rn measurements. Because the indoor ^{222}Rn concentrations in the soil was low, indoor concentrations were consistent with outdoor air. Instead we compared the ^{222}Rn concentrations in the sub-slab and deep soil to estimate the rate of ^{222}Rn removal from the sub-slab soil-gas into the building. This comparison assumed that ^{222}Rn was 1) supplied to both regions with equal emanation rates, 2) removed from the deep soil gas only by radioactive decay, and 3) removed from the sub-slab soil gas by both radioactive decay and transport into the building. Assumption 1) is justified because the soil is all from the same parent material and has approximately constant moisture content (25), 2) is justified because the concentration gradients are too small to drive strong diffusive flow into the sub-slab region, and because the upwind-downwind advective flows are very slow . If no significant removal other than

13

natural radioactive decay occurs in the deep soil, then the concentration in the deep soil will be a balance between the rates for emanation from the soil and radioactive decay: C_{Rn} (deep) = E/λ, where E is the emanation rate (Bq m^{-3} s^{-1}), and λ = 0.18 d^{-1} is the radioactive decay rate for ^{222}Rn. In the sub-slab area, soil-gas entry adds another removal rate and the concentration will be lower: C_{Rn} (subslab) = E' /(λ + Q_{eff} /V_{ss}) , where the sub-slab air volume V_{ss} = ε_a A Δz $\approx$ 5 m^3. Using the measured ratio of deep to subslab ^{222}Rn concentrations, C_{Rn} (deep) / C_{Rn}(subslab) = 1.9±0.3 , the effective flow Q_{eff} $\approx$ 0.8 m^3 d^{-1}. This is in general agreement with the estimate obtained from the tracer-gas measurements.

Effective soil-gas entry rates were estimated as a function of building depressurization using the measured SF$_6$ concentrations and Eqs (1) and (2). The results are shown in Figure 7 for the estimate of ambient conditions and for imposed depressurizations of 10 and 75 Pa (shown as filled circles). Because measurements of the building depressurization under ambient conditions were not made, the effective entry rate under ambient conditions (shown as a hatched region in Figure 7) is estimated from the one week average of indoor SF$_6$ concentrations, assuming a range of depressurizations between 1 and 4 Pa. The dependence of the soil-gas entry rate on building depressurization is approximately linear (see thick solid line in Figure 7), in agreement with a model for advective soil-gas entry limited by the soil permeability to air rather (26), although the available data can not discriminate against small deviations from linearity.

We note that the data shown in Figure 7 yield an underestimate the slope due to purely advective entry because advection increases with ΔP whereas diffusion does not. The size of the diffusive component can be estimated very approximately by considering diffusion through the concrete slab. Fick's law for diffusion yields an the flux density for diffusive transport of a gas species

$$J_{dif} = - D_e \, dC/dz, \tag{5}$$

where D_e is the effective diffusivity. Applying Eq (4) to the case of a concrete slab, the contribution to diffusive entry is A J_{dif} $\approx$ A D_e C(subslab)/t $\approx$ C(subslab) x 0.4 m^3 d^{-1}, where

the diffusivity (for ^{222}Rn and approximately that for other gases) in concrete $D_e = 8.6 \times 10^{-4} \, m^2$ d^{-1} (27), and t = 0.1m is the thickness of the building slab. Thus, the equivalent entry rate due to diffusion of $0.4 \, m^3 \, d^{-1}$ is roughly half of the total entry rate at low pressures but becomes insignificant at larger depressurizations.

Estimated rate of vertical diffusive transport

Two methods were employed to estimate the rate of vertical transport across the low diffusivity layer in the soil. The first assumed mass balance between the vertical transport from the deep soil gas into the sub-slab soil gas and the subslab removal (building entry) estimated above. In this case, the flow of SF_6 into the sub-slab region

$$F_{SF6} = Q_{eff} \, C_{SF6}(subslab) \approx 20 - 60 \, ppb \, m^3 \, d^{-1}, \qquad (6)$$

where $C_{SF6}(subslab) = 20$ ppb is the average SF_6 concentration measured in shallow subslab probes 50 days after the tracer gas injection when the concentrations in the shallow soil have reached conditions close to steady state (see Figure 3).

The second method estimates the vertical diffusive transport from the measured air-filled soil porosity and the gradient in gas concentration using Fick's law from Eq (2). The effective diffusivity in the soil is assumed to follow the form derived by Millington and Quirk (28):

$$D_e = D_0 \, (\varepsilon_a^{10/3}/\varepsilon^2), \qquad (7)$$

where D_0 is the molecular diffusivity for the gas in question, and ε_a and ε are the air-filled and total porosities. For SF_6, $D_0 \, (SF_6) = 0.088 \, cm^2 \, s^{-1}$ (29), the effective diffusivity in the soil $D_e \approx 0.76 \, m^2 \, d^{-1} \, (0.2)^{3.333}/(0.4)^2 \approx 0.02 \, m^2 \, d^{-1}$, and the SF_6 gradient across the depth interval from 0.4 to 0.65 m $dC_{SF6}/dz \approx \Delta C_{SF6}/\Delta z \approx (30 \, ppb - 400 \, ppb) / (0.25 \, m) \approx -1500 \, ppb \, m^{-1}$. The resulting estimated flow of SF_6 into the sub-slab region

$$J_{dif} \, A \approx 1500 \, ppb \, m^3 \, d^{-1}, \qquad (8)$$

is 25 to 75 times greater than that estimated from the subslab ventilation in Eq (6). This suggests that either the estimated rate of removal from the sub-slab region is inaccurate, or, as we believe more likely, that the soil at depths between 0.4 and 0.65 m contains a thin layer with very low diffusivity that was not detected by the soil-core measurements. For example, a layer of

saturated soil only 2 mm thick would decrease the diffusive transport by an order of magnitude. One piece of evidence weakly supports this hypothesis; the measured water content shows a significant increase in the layer between 0.4 and 0.6 m (see Table 2).

We also compared the SF_6 transport observed in the soil at depths > 0.65 m to the results of a model for soil gas transport that contains no fitted parameters. We assumed that: 1) the SF_6 could be treated as a Gaussian puff that was transported by the combined effects of diffusion and advection in a soil layer bounded from below by the water table at 2 m and from above by a layer of low diffusivity soil at 0.5 m, and 2) the advective flow was that estimated in Eq (3). The transport of a Gaussian puff in free air is described in Seinfeld (30). We applied that solution to this problem by scaling the concentration of the SF_6 puff by the inverse of the air-filled pore space, and using the soil-core data and Eq (7) to estimate the diffusivity in the deep soil. The results of this calculation (lines) are compared with the measured concentration data (points) for each of the deep probes in Figure 4. We note both the maximum concentration and the time at which the maximum is reached depend on the horizontal distance from the source and the orientation of the source and detector relative to the direction of advective flow. The model agrees with the measurements to within a factor of two for most of the data. Given the limited number of parameters (all of which are fixed) and the fact that heterogeneity should be expected in subsurface systems, the observed level of agreement between the measurements and the model predictions largely substantiates this description of transport in the soil.

Estimated rate of hydrocarbon biodegradation

Independent of the rate of subslab ventilation, the very sharp concentration gradient observed in the VOC's relative to SF_6 suggests that something qualitatively different was affecting VOC transport. To elaborate, the ratios of soil-gas concentrations measured at depths between 0.65 and 0.1 m was ≈ 1000 for isoP, while the corresponding ratio was ≈ 40 for SF_6. Non-steady state conditions are not likely to be the cause of this difference. The isoP gradient was consistently large over the course of the year-long series of measurements, and the measured SF_6 gradient clearly approached a steady-state ratio (Figure 3).

Several pieces of evidence suggest that biodegradation is responsible for the sharper concentration gradient observed in isoP relative to SF_6. First, we estimated the stoichiometry of the reactions occurring in the soil from the measured gradients in isoP, CH_4, and O_2 assuming that the flux rates were governed by diffusive transport. The CO_2 gradient was not included in the analysis because the high pH of the soil was indicative that carbonate chemistry would significantly affect the CO_2 concentrations. The diffusivity of each gas relative to O_2 was estimated by the ratio of their molecular diffusivities ($D_0(isoP) = 0.09$ cm^2 s^{-1}, $D_0(CH_4) = 0.23$ cm^2 s^{-1}), to that of O_2 ($D_0(O_2) = 0.2$ cm^2 s^{-1}) (31). If we assume that half of the carbon consumed was converted to microbial biomass (21) and that little mineralization (to CO_2) of inactive biomass occurred, then the required ratio of molar flow rates of O_2 relative to isoP and CH_4 are 4 and 1. Under these assumptions the balance between VOC consumption and O_2 supply matches to within 10%. Further, the maximum imbalance in the flux of O_2 to the combined fluxes of isoP and CH_4 is only a factor of two if one assumes that the amount of biomass is in steady state and that production of new biomass is balanced by mineralization of inactive biomass.

Second, we estimate the rates of isoP and CH_4 degradation necessary to produce the observed concentration gradients. We assume that the rate of degradation must approximately equal the total flux rates because the gradients were much larger than that for SF_6 where no degradation occurred. Diffusive flux rates were calculated using the measured gradients and the estimated rate of soil gas transport across the soil layer between 0.4 and 0.65 m. The gradients were calculated as $\Delta C_{VOC}/\Delta z$, where ΔC_{VOC} is the difference in concentration measured between the probes at 0.4 and 0.65 m (see Figure 2), and $\Delta z = 0.25$ m. The minimum effective diffusivity for SF_6 is estimated, assuming the mass balance between diffusion from deep soil-gas into (see Eq (5)), and building entry removal (see Eq (6)) out of the sub-slab region, as

$$D_e(SF_6) = F_{SF6}/A \ \Delta C_{SF6}/\Delta z \approx 3 \times 10^{-4} \text{ m}^2 \text{ d}^{-1}, \tag{9}$$

where $\Delta C_{SF6}/\Delta z$ is the SF_6 gradient across that layer of soil. The maximum effective diffusivity, estimated from the porosity measurements (see Eq (7)) of bulk soil, is 80 times greater. The

flux density for a given VOC is given by Eq (3) with a diffusivity scaled from Eq (9) using the ratio of molecular diffusivities:

$$J_{VOC} = D_e(SF_6) \, D_0(VOC)/D_0(SF_6) \, \Delta C_{VOC}/\Delta z. \qquad (10)$$

The range of degradation rate per unit mass of soil is then estimated to be

$$K = (J_{isoP} + J_{CH4}) / \rho \, \Delta z \approx 0.5\text{-}40 \, \mu g \; VOC/g \; soil \; d^{-1}, \qquad (11)$$

where the range of values reflects the range of $D_e(SF_6)$ used in Eq(10).

Third, we compared the results of the laboratory isoP degradation experiments with the rates estimated above. The best fit exponential decay curves for the isoP concentrations are shown in Figure 5. The time constants for consumption of isoP in the soil samples collected at depths of 0.2-0.4 and 0.5-0.7 m are $\tau = 80$ and 265 hr respectively. These correspond to degradation rates $K_{lab} = \Delta M_{isoP} / (\tau \, M_{soil}) = 110 - 380 \, \mu g \; VOC/g \; soil \; d^{-1}$, where ΔM_{isoP} and M_{soil} are the masses of isoP consumed and moist soil respectively. These values are considerably higher than the rates estimated from the field measurements. This suggests that the rate of *in-situ* microbial VOC degradation was subject to some combination of substrate, nutrient, and/or oxygen limitations. Because nutrient availability can be assumed to be approximately the same in the laboratory samples as in the bulk soil, substrate and/or oxygen limitations were the more likely causes.

Last, we consider whether the low-diffusivity layer could have been caused by reduced soil porosity due to an accumulation of microbial biomass with it's associated protective layers of polysaccharides and water. Analogous examples of biomass mediated reductions in transport are the large reductions of hydraulic conductivity found in saturated systems (32, 33). In the case of this study, if the soil pores were filled with biotic material with typical water content (~70% H_2O to ~30% organic) then the minimum soil organic fraction would be $f_{oc} = 0.08$. This appears unlikely because the measured fraction of organic material in the bulk soil at depths between 0.4 - 0.65 m is $f_{oc} \approx 0.005$, although an unknown amount of volatile carbon may have been lost when the soils samples were dried. Also, in a separate study at this site, Conrad et al. (34) show that the ^{14}C content of the organic matter in the soil samples from the 0.4 to 0.65 m layer contained a

[14]C fraction of 0.8 relative to the ^{14}C content of the atmosphere before above-ground nuclear tests were conducted (the present-day fraction of ^{14}C is 1.14). An upper limit on the soil carbon derived from ancient hydrocarbons (which contain no ^{14}C), estimated by assuming all the measured ^{14}C comes from material with a ^{14}C fraction of 1.0, is f_{oc}(petroleum) ≈ 0.001, although again this could be larger if organic carbon lost during soil drying was predominantly derived from petroleum.

Discussion

The results of this study demonstrate that the indoor air concentrations of gasoline hydrocarbons were significantly lower than what would be expected based on the estimates of building ventilation and the entry of soil gas containing concentrations of VOC's measured in the soil less than a meter under the building. Analysis of the measurements suggest that a combination of physical and biological factors reduced the soil gas VOC concentrations at the building slab by a factor of 1000 compared with those below 0.65 m. In this section we discuss these results, the connections between the physical and biological factors, and the degree to which similar phenomena might occur at other sites.

First, the estimated rates of hydrocarbon degradation from Eq(11) are consistent with measurements reported by Hinchee & Ong for *in-situ* hydrocarbon degradation in contaminated soils, where K = 0.4 - 20 μg VOC/g soil d[-1] (21). Second, Conrad et al. (34) found that the CO_2 in the soil gas contained stable isotope (^{13}C/^{12}C) and radiocarbon (^{14}C/^{12}C) ratios that were both suggestive of microbial consumption of petroleum hydrocarbons. Thus, while we find several consistent pieces of evidence for biodegradation, we are unable to find a completely satisfying explanation for the low diffusivity layer between depths of 0.4 and 0.65 m.

Finally, the effects of physical reduction in soil gas transport and microbial degradation of contaminants are likely to affect indoor air concentrations of contaminants to varying degrees at other sites. In particular, although near-surface aerobic biodegradation of aliphatic petroleum hydrocarbons may occur faster than the biodegradation of other compounds in less aerobic environments (particularly halogenated hydrocarbons in the deep subsurface), similar types of

effects may be observed. Finally, these results suggest that attempts to make detailed estimates of VOC transport into buildings should be made with careful attention to the identification and separation of physical and biotic effects.

Acknowledgments

Literature Cited

(1) Kliest, J.; Fast, T.; Bolij, J. S. M.; van de Wiel, H.; Bloemen, H. Environment International 1989, 15, 419-425.

(2) Wood, J. A.; Porter, M. L. Journal of the Air Pollution Control Association 1987, 37, 609-615.

(3) Garbesi, K. Lawrence Berkeley National Laboratory Report No. LBL-25519; University of California: Berkeley, CA, 1988.

(4) Hodgson, A. T.; Garbesi, K.; Sextro, R. G.; Daisey, J. M. Journal of the Air and Waste Management Association 1992, 42, 277-283.

(5) EPA Report No. EPA/625/6-87-015; U. S. Environmental Protection Agency 1987.

(6) Kullman, G. J.; Hill, R. A. Appl. Occup. Environ. Hyg. 1990, 5, 36-37.

(7) Moseley, C. L.; Meyer, M. R. Environ. Sci. Technol. 1992, 26, 185-192.

(8) Johnson, P. C.; Ettinger, R. A. Environ. Sci. Technol. 1991, 25, 1445-1452.

(9) Little, J. C.; Daisey, J. M.; Nazaroff, W. W. Environ. Sci. Technol. 1992, 26, 2058-2066.

(10) Sanders, P. F.; Stern, A. H. Env. Tox. Chem. 1994, 13, 1367-1373.

(11) Westbrook, W. Report No. EPA-451/R-92-002; US EPA: Washington, DC, 1992.

(12) ANAS Report No. reports compiled by the Office of Environmental Protection, Alameda Naval Air Station: Alameda, CA, 1995.

(13) ST-032, Envirochem Inc.

(14) Scheff, P.; Wadden, R.; Bates, B.; Aronian, P. JAPCA 1989, 39, 469-478.

(15) Carter, M. R., ed. *Soil Sampling and Methods of Analysis.* , Lewis: Boca Raton, 1993.

(16) Turk, B. H.; Prill, R. J.; Grimsrud, D. T.; Moed, B. A.; Sextro, R. G. Lawrence Berkeley National Laboratory Report No. LBL-23430; University of California: Berkeley, CA, 1987.

(17) Garbesi, K.; Sextro, R. G.; Robinson, A. L.; Wooley, J. D.; Owens, J. A.; Nazaroff, W. W. Water Resources Res. 1995, (in press).

(18) McDonald, M., (private communication), 1994.

(19) Turk, B. H.; Harrison, J.; Prill, R. J.; Sextro, R. G. Health Physics 1990, 59, 405-419.

(20) E779-87, *Test Method for Determining Air Leakage by Fan Presurization*, in *ASTM Book of Standards*, American Society of Testing and Materials, 1991.

(21) Hinchee, R. E.; Ong, S. K. J. Air Waste Management 1992, 42, 1305-1312.

(22) Robinson, A. L.; Sextro, R. G. Geo. Res. Lett. 1995, 22, 1929-1932.

(23) Riley, W. J.; Gadgil, A. J.; Bonnefous, Y. C.; Nazaroff, W. W. Atmos. Env. 1995, (in press).

(24) Allen, C. Report No. AIC 13; International Energy Agency/ Air Infiltration Centre; Berkshire, UK. 1984.

(25) Nazaroff, W. W. Reviews of Geophysics 1992, 30, 137-160.

(26) Garbesi, K. Sextro, R. G. Environ. Sci. Technol. 1989, 23, 1481-1487.

(27) Revzan, K. L.; Fisk, W. J.; Sextro, R. G. Health Physics 1992, 65, 375-385.

(28) Millington, R. J. Quirk, J. M. Trans. Faraday Soc. 1961, 57, 1200-1207.

(29) Suetin, P. E. Ivakin, B. A. Sov. Phys.-Tech. Phys. 1961, 6, 359-361.

(30) Seinfeld, J. H. *Atmospheric Chemistry and Physics of Air Pollution*, New York: John
Wiley & Sons, 1986.

(31) Schwartzenbach, R. P.; Gschwend, P. M.; Imboden, D. M.*Environmental Organic
Chemistry*, New York: Wiley-Interscience, 1993.

(32) Taylor, S. W. Jaffe, P. L. Water Resources Res. 1990, 26, 2153-2159.

(33) Vandevivere, P. Baveye, P. Applied Environmental Microbiology 1992, 58, 2523-2530.

(34) Conrad, M. E.; Daley, P. F.; Fischer, M. L.; Buchanan, B. B.; Leighton, T.; Kashgarian,
M. Nature 1995, (submitted).

TABLES

Table 1   Compounds detected in air, soil gas , and water headspace samples.

Compound	Outdoor Air	Indoor Air	Soil gas (0.1m)	Soil gas (0.7 m)	Water Headspace (2 m)
	(μg m^{-3})			(mg m^{-3})	
Isopentane (isoP)	11.3	36.6	25	27500	143000
n-Pentane	5.2	5.4	6.3	2000	53000
2-Methylpentane	5.6	5.5	3.4	6700	79000
3-Methylpentane	2.9	2.1	2.2	ND	31000
2,3-Dimethylpentane	2.7	3.6	2.4	2000	ND
3-Methylhexane	1.1	1.5	0.5	260	12000
4-Methylhexane	1.3	1.9	1.3	1400	4600
Benzene	1.2	2.9	0.5	100	8000
Toluene	5.8	5.7	2	ND	8000
Detection limit[*]	0.33	0.33	0.2	50	100

[*] Detection limit is approximately 1 ng divided by the sample volume. Benzene detection limits are approximately 3-6 times greater due to the presence of a 3-6 ng benzene background from the Tenax sorbent. ND indicates no significant detection.

Table 2 Soil properties.

Depth (m)	Density ρ (10^3 kg/m^3)	Total Porosity ε	Air filled Porosity ε_a	Clay* Fraction (g/100g)	Silt* Fraction (g/100g)	Organic Carbon f_{oc} (g/100g)	Moisture Content (g/100g)
0.2	1.6	0.37	0.24	6.5	2.2	0.4	8
0.38	1.6	0.37	0.23	8	-0.3	0.30	8
0.48	1.7	0.33	0.21	2.7	1.5	0.1	7
0.58	1.6	0.38	0.21	5.9	1.5	0.4	11
0.62	1.5	0.39	0.19	3.3	3.6	0.5	13
0.70	1.6	0.34	0.16	3.6	3.4	0.6	10
0.95	1.6	0.39	0.26	3.8	2.2	0.07	7
1.14	1.6	0.38	0.26	-0.9	6.9	0.06	7
1.35	1.5	0.41	0.26	-0.3	5.2	0.06	9
1.60	1.4	0.46	0.18	-0.9	5.0	0.08	19
1.95	1.3	0.51	0.08	26.5	12.2	0.07	32

* Negative values indicate noise level of measurements. Mass of clay, silt, and organic carbon, and moisture are reported relative to mass of dry soil. Remainder of soil is sand.

Table 3 Changes in concentrations during soil incubation [*]

Sample	ΔisoP	ΔCO_2	ΔO_2
	mole m^{-3}		
Blanks	0.03 (0.02)	0.05 (0.04)	-2.0 (0.04)
Sterile Soil Control (0.2-0.4 m)	-0.01	0.1	-0.7
Sterile Soil Control (0.5-0.7 m)	-0.03	0.05	-0.6
Soil (0.2-0.4 m)	-0.67 (0.01)	1.6 (0.08)	-2.9 (0.1)
Soil (0.5-0.7 m)	-0.5 (0.04)	1.1 (0.05)	-2.4 (0.1)

[*] Assumes initial concentrations of isoP, CO_2, and O_2 are 0.7 (50 g m^{-3}), 0.01 (350 ppm), and 8.8 moles m^{-3} (21%) respectively. Time duration of experiment was 450 hr. Standard errors of measurements given in parentheses where available.
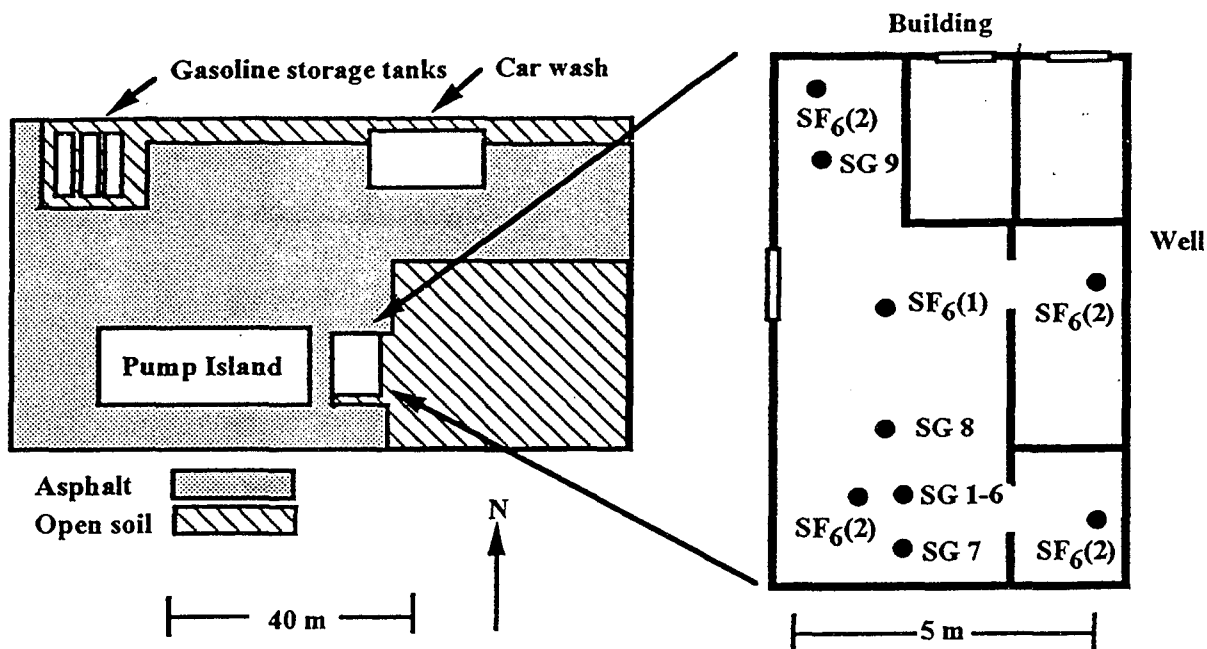
Figure 1. Site geometry and enlarged planar view of service station building showing locations of soil gas probes (e.g., SG 8) and the locations of the injections used for the two tracer gas tests $SF_6(1)$ and $SF_6(2)$. A cluster of six probes, installed at depths ranging from 0.1 to 1.65 m is marked as SG 1-6. A well used to monitor ground water depth is also shown.
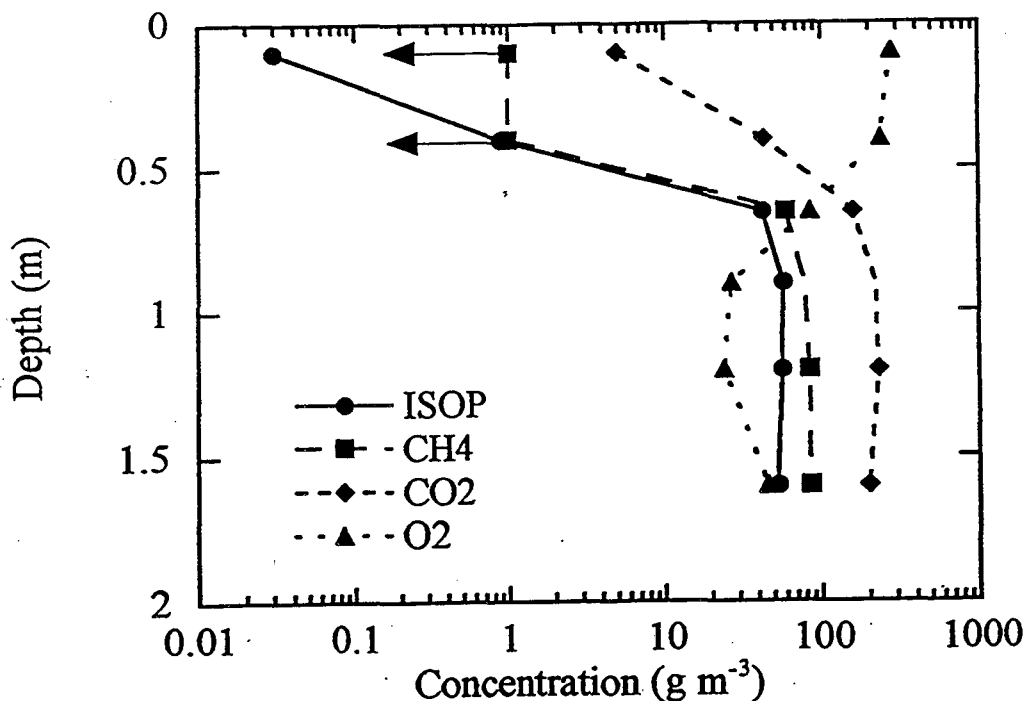

Figure 2. Concentrations of isoP, CH_4, CO_2, and O_2 in soil gas as a function of depth. Arrows indicate detection limit for CH_4, which was not detected in the soil gas at depths of 0.1 and 0.4 m. Note the sharp gradients in all gas species at depths between 0.1 and 0.65 m.
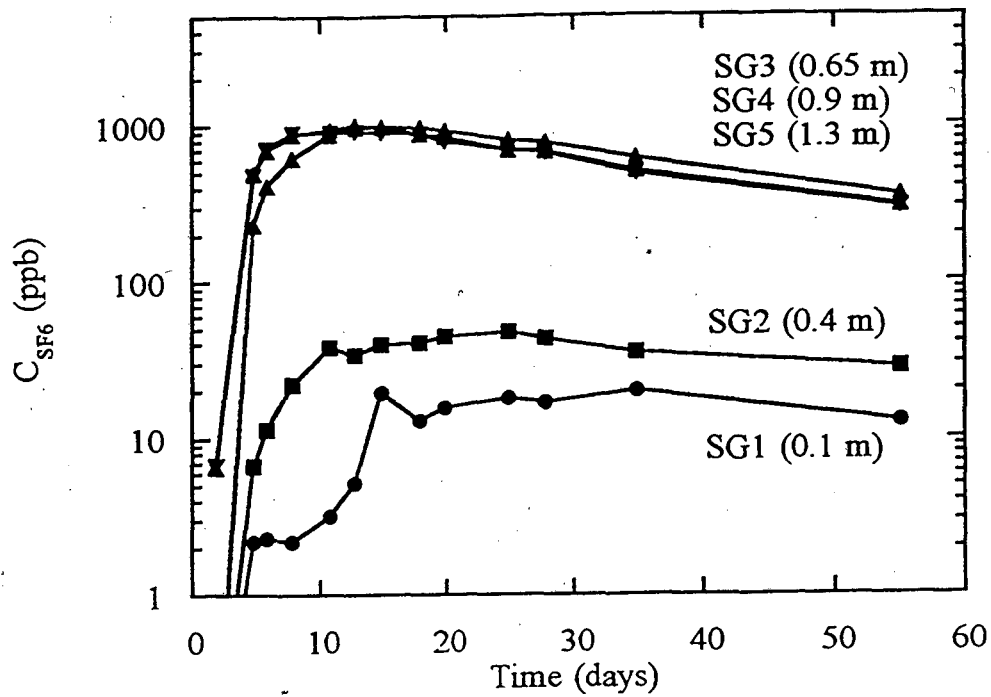
26

Figure 3. SF₆ concentrations at fixed horizonal distance vs. time during first tracer gas transport test. Concentrations are those measured in a cluster of probes (SG 1 to SG 6) that are at the same horizontal distance from the source but at varying depths (indicated in parentheses). A sharp gradient (note logarithmic scale) is observed with depth, similar to that found for the VOC, suggesting the existence of a partial barrier to vertical transport. Lines simply connect data points to guide the eye.
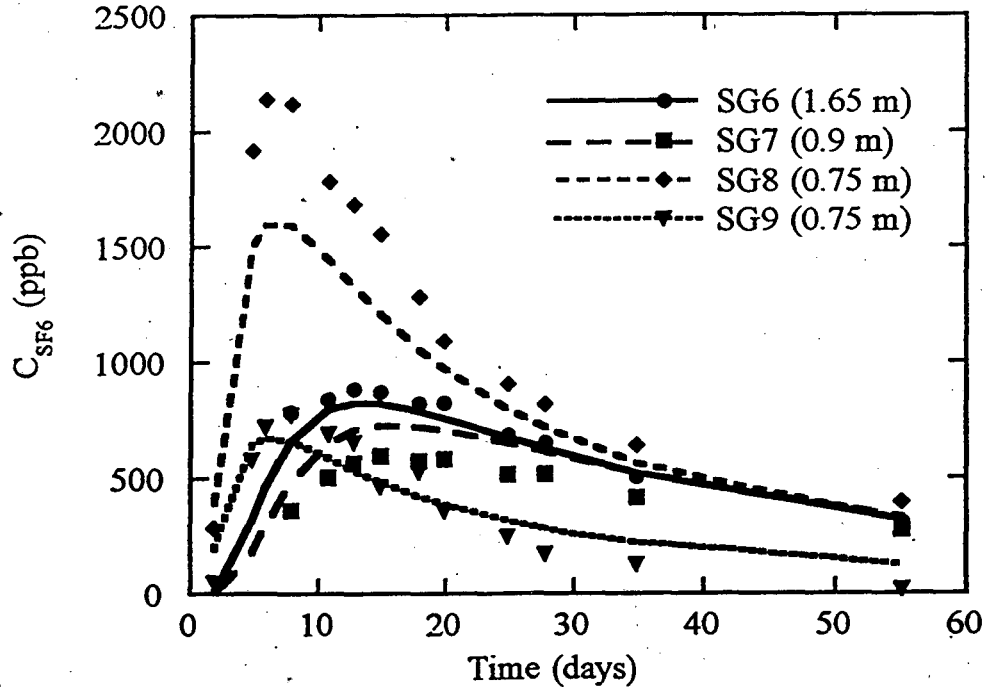

Figure 4. Comparison of measured and modeled SF₆ concentrations in deep soil probes vs. time for first tracer gas transport test. Concentration data (points) are those measured in probes located at depths greater than 0.65 m and at varying horizontal distances from the SF₆(1) source injection point (see Figure 1). Results of model calculation are shown as separate lines for each probe location.
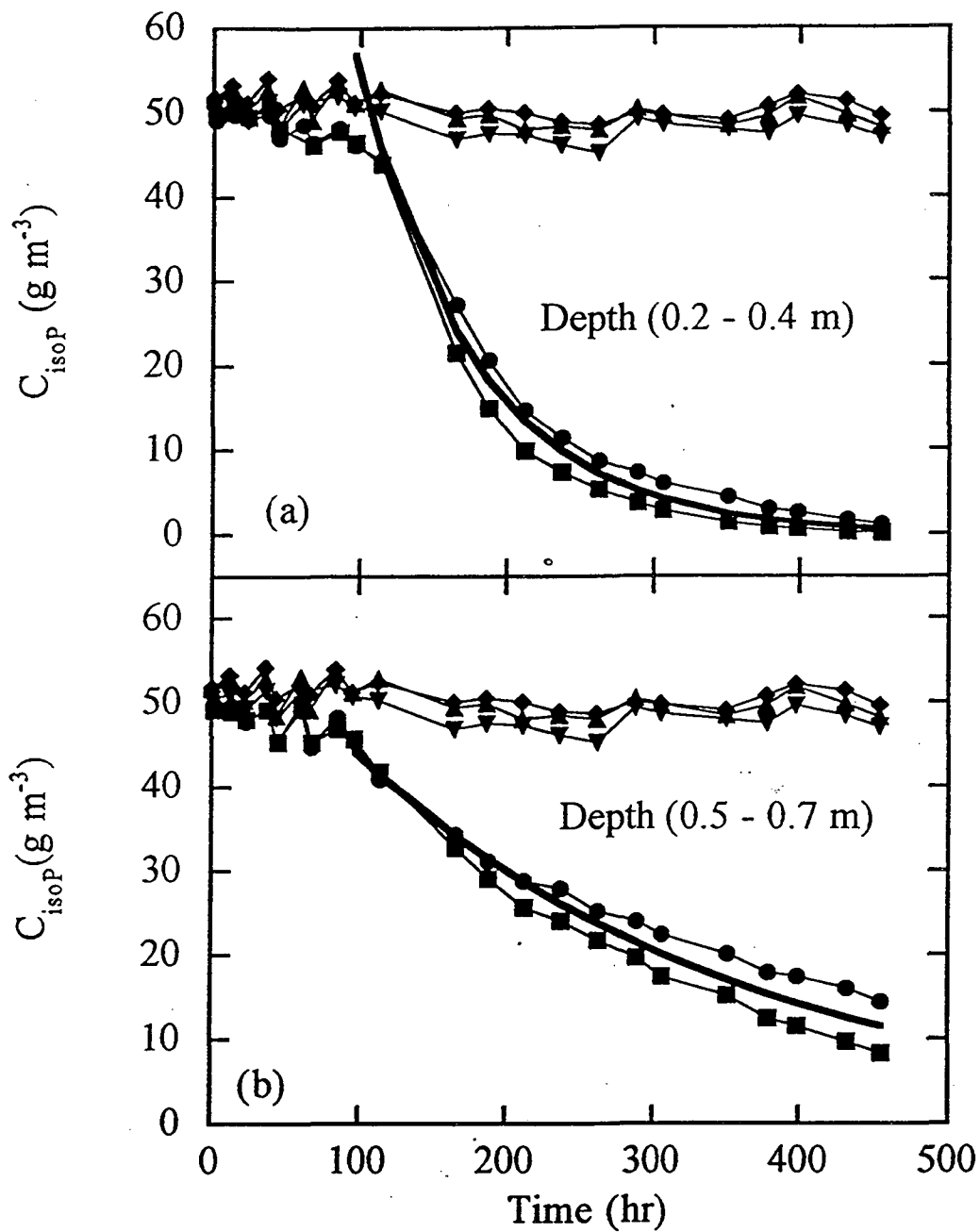
Figure 5. Headspace concentrations of isoP as a function of time during laboratory incubation. Data shown are blank controls (triangles), sterilized soil controls (diamonds), and active soil samples (circles and squares). Panels (a) and (b) show the results for soil samples collected from under the building at depths of 0.2-0.4 and 0.5-0.7 m respectively. Best fit exponential decay curves (thick lines) are fit to the data for active soil samples. The delay (lag phase) between initiation of the experiment and time for measurable decay of isoP in the active soil samples is attributed to the time required for significant growth in the bacterial population.

Schematic of Model for Transport

Equivalent Box Model

Wind Loading

Building Depressurization
Pout - Pin ≈ 1 - 4 Pa

Advection of sub-slab soil gas into building

Diffusion of sub-slab soil gas into building

Biodegradation

Low diffusivity layer

Upwind-downwind Advection in soil gas   **Diffusion from deep to sub-slab soil gas**

Water Table

Outdoor Air C(outdoor)

Indoor Air C(indoor)

Advection   **Diffusion**

Sub-slab soil gas C(subslab)

Upwind-downwind Advection

Biodegradation

Diffusion

Deep soil gas C(deep)
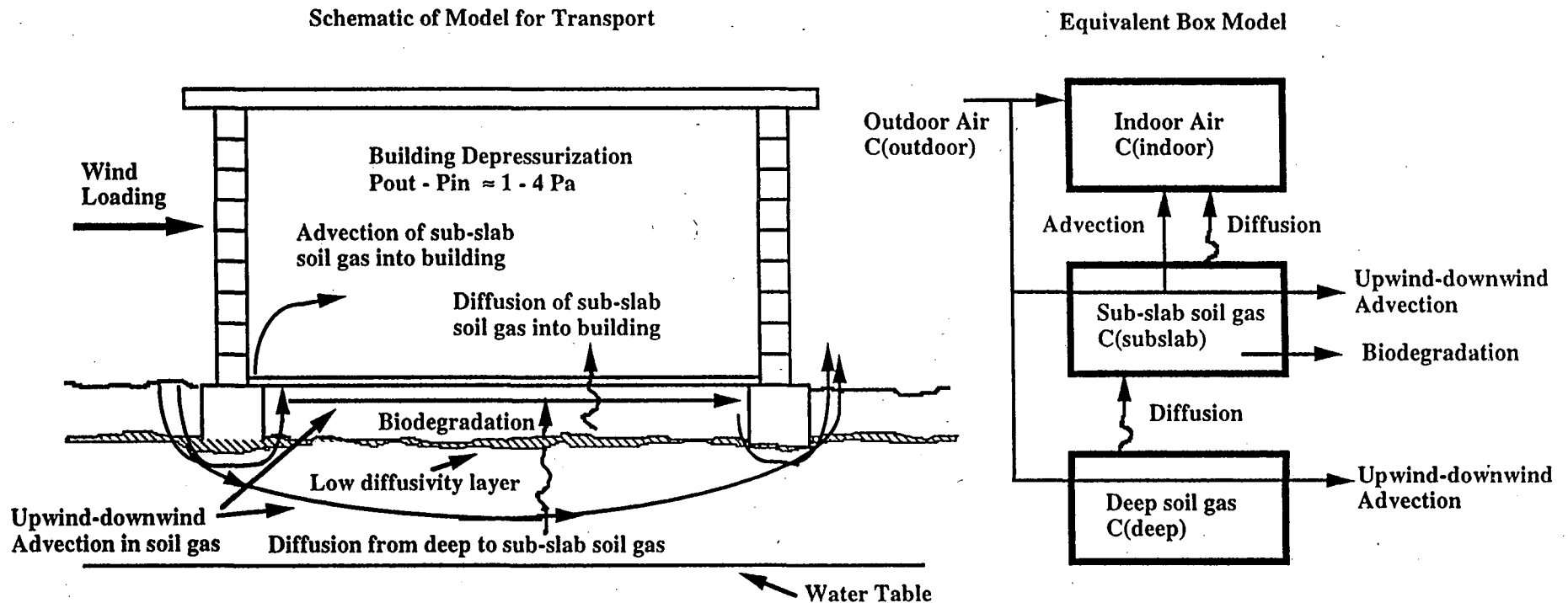
Upwind-downwind Advection

Figure 6. Schematic of model for soil gas transport into the building and equivalent three box model. Contaminant transport is assumed to occur by diffusion from the deep soil, through the subslab region, and into the building. At depths between 0.4 and 0.65 m a low diffusivity layer restricts the flow generating a sharp gradient in the contaminants, CO_2, and O_2. In and above the layer, an aerobic microbial population consumes a fraction of the contaminants that cross the layer. The remaining contaminants are transported into the building from the sub-slab region by 1) outdoor air driven into the soil and by depressurization caused by wind loading on the building, and 2) diffusion though the building slab. Wind loading on the building also generates low-velocity "upwind-downwind" advective flow in the soil gas from the upwind to downwind sides of the building.
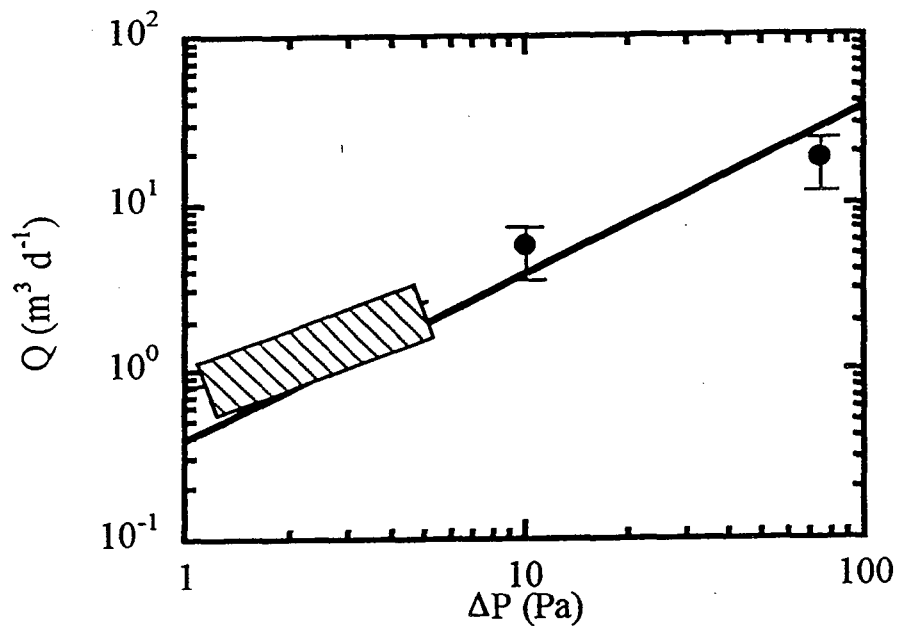
Figure 7. Measured soil-gas entry rate into the building as a function of building depressurization. The entry rate estimated for the case of ambient conditions (shown as the hatched region) assumed an ambient depressurization between 1 and 4 Pa caused by wind loading on the building. The entry rates estimated from imposed depressurizations of 10 and 75 Pa are shown as points with standard errors. The flow rate is approximately proportional (thick line) to depressurization , although the data can not be used to rule out small departures from linearity.

LAWRENCE BERKELEY LABORATORY
UNIVERSITY OF CALIFORNIA
TECHNICAL AND ELECTRONIC
  INFORMATION DEPARTMENT
BERKELEY, CALIFORNIA 94720